



# CDC20 inhibition alleviates fibrotic response of renal tubular epithelial cells and fibroblasts by regulating nuclear translocation of $\beta$ -catenin

Jia He<sup>a,b,1</sup>, Shuang Xu<sup>a,b,1</sup>, Mingzhu Jiang<sup>a,b</sup>, Ting Wang<sup>a,b</sup>, Yue Zhang<sup>a,b</sup>, Zhanjun Jia<sup>a,b,c,\*</sup>, Mi Bai<sup>a,b,c,\*</sup>, Aihua Zhang<sup>a,b,c,\*</sup>

<sup>a</sup> Department of Nephrology, State Key Laboratory of Reproductive Medicine, Children's Hospital of Nanjing Medical University, Nanjing 211166, China

<sup>b</sup> Jiangsu Key Laboratory of Pediatrics, Nanjing Medical University, Nanjing 210029, China

<sup>c</sup> Nanjing Key Laboratory of Pediatrics, Children's Hospital of Nanjing Medical University, Nanjing 210008, China

## ARTICLE INFO

### Keywords:

CDC20  
Tubular epithelial cells  
Fibroblasts  
 $\beta$ -Catenin  
Renal fibrosis

## ABSTRACT

Fibrosis is a common pathological phenomenon in progressive kidney disease leading to eventual loss of kidney function. Previous studies demonstrated that CDC20 plays a role in cancers by regulating epithelial-mesenchymal transition (EMT) and the infiltration of fibroblasts, suggesting the potential of CDC20 in regulating fibrotic response. However, the role of CDC20 in renal fibrosis is yet unclear. Herein, we reported that renal CDC20 was remarkably upregulated in renal tubular epithelial cells and fibroblasts in chronic kidney disease (CKD) patients, which was in line with a positive correlation with the severity of kidney fibrosis. In mice with unilateral urinary obstruction, CDC20 was also strikingly enhanced, and treatment with Apclin, an inhibitor of CDC20, ameliorated kidney fibrosis. Consistently, the pharmacological inhibition of CDC20 in mouse proximal tubular epithelial cells and rat fibroblasts attenuated TGF- $\beta$ 1-induced fibrotic responses, while overexpression of CDC20 aggravated such responses. Additional studies revealed that CDC20 induces nuclear translocation of  $\beta$ -catenin, which in turn initiates and promotes the pathological process of fibrosis in CKD. Thus, enhanced CDC20 in renal tubular cells and fibroblasts promotes renal fibrosis by activating  $\beta$ -catenin, and CDC20 inhibition may serve as a promising strategy for the prevention and treatment of renal fibrosis.

## 1. Introduction

Chronic kidney disease (CKD) has been recognized as a leading global public health burden with an estimated prevalence of >10 % [1]. It involves an irreversible change in the function or structure of the kidney and is characterized by a slow progression [2]. Several factors contributed to CKD progression, including parenchymal cell loss, chronic inflammation, reduced regenerative capacity of the kidney, and renal fibrosis [3,4]. Renal fibrosis, especially tubulointerstitial fibrosis, is an inevitable and progressive process that occurs in almost every type of CKD. It is characterized by profound remodeling and excessive production/deposition of fibrillar extracellular matrix (ECM) [5]. The current therapeutic options for CKD in the clinical setting are scarce and delay the progression of the disease. An approved treatment specifically targeted to renal fibrosis is almost nonexistent. Thus, the optimization of treatment should be based on an improved understanding of the

pathogenesis of renal fibrosis.

Cell-division cycle protein 20 homolog (CDC20) is a highly conserved activator of the anaphase-promoting complex/cyclosome, which plays a critical role in governing mitotic progression by targeting key cell cycle regulators for degradation [6]. The high expression of CDC20 has been reported in many types of malignant tumors [7,8]. It participates in the occurrence and development of tumors by regulating mitotic progression and apoptosis [9–11]. In addition to its canonical role in cell cycle regulation, recent studies have demonstrated that CDC20 participates in many cellular processes, including embryo implantation, ciliary formation, osteogenic commitment, or DNA damage repair [12–15]. The role of CDC20 in fibrosis has also been demonstrated in several recent studies. The integrated pan-cancer analysis in human tumors showed that for most cancer types, CDC20 expression is positively correlated with the infiltration of cancer-associated fibroblasts [16]. Epithelial-mesenchymal transition (EMT) is defined as a

\* Corresponding authors at: Department of Nephrology, State Key Laboratory of Reproductive Medicine, Children's Hospital of Nanjing Medical University, 72 Guangzhou Road, Nanjing 210008, China.

E-mail addresses: [jiajz72@hotmail.com](mailto:jiajz72@hotmail.com) (Z. Jia), [baimi3@njmu.edu.cn](mailto:baimi3@njmu.edu.cn) (M. Bai), [zhaihua@njmu.edu.cn](mailto:zhaihua@njmu.edu.cn) (A. Zhang).

<sup>1</sup> These authors contributed equally to this work.

<https://doi.org/10.1016/j.bbadis.2023.166663>

Received 6 December 2022; Received in revised form 2 February 2023; Accepted 4 February 2023

Available online 9 February 2023

0925-4439/© 2023 Elsevier B.V. All rights reserved.

process in which differentiated epithelial cells undergo phenotypic transformation into myofibroblasts capable of producing ECM, and it is regarded as an integral part of renal fibrogenesis [17]. CDC20 silencing inhibits cancer cell growth and alleviates drug resistance by preventing EMT in various cancer cells [18–20]. These data implicated multiple functions of CDC20 in cellular processes and its potential role in fibrosis.

However, the role of CDC20 in renal fibrosis has not yet been characterized. Next, we examined the expression of CDC20 in human patients and mice with renal fibrosis. Apcin, a small molecule that binds to CDC20 and competitively inhibits the ubiquitination of D-box-containing substrate [21] was used to examine the role of CDC20 silencing in renal fibrosis. The present study indicated that Apcin treatment dramatically attenuates the ECM accumulation and the activation of fibroblasts in the obstructed kidney tissues and tumor growth factor- $\beta$ 1 (TGF- $\beta$ 1)-stimulated cells, whereas these outcomes were aggravated by CDC20 overexpression. Further studies indicated that CDC20 upregulation was concomitant with the activation of  $\beta$ -catenin signaling, which is crucial for promoting renal fibrosis in CKD. The current data suggested a vital role of CDC20 in the progression of renal fibrosis; thus, the inhibition of CDC20 is a potential novel therapy to antagonize renal fibrosis.

2. Materials and methods

2.1. Reagents and antibodies

DMEM, DMEM/F-12, and fetal bovine serum (FBS) were purchased from Gibco (Waltham, MA, USA). Apcin (HY-110287) and Cell Counting Kit-8 (CCK-8, HY-K0301) were purchased from MedChemExpress (Shanghai, China). jetPRIME® (101000046) from Ployplus (Illkirch, France) was selected as the transfection reagent. Antibodies for fibronectin 1 (FN1, ab2413) and  $\alpha$ -smooth muscle actin ( $\alpha$ -SMA, ab7817) were from Abcam (Cambridge, MA); Collagen I (bs-10423R) and Collagen III (bs-0549R) antibodies were from Bioss (Beijing, China); anti-CDC20 (A15656), anti-Snail (A11794), anti-Histone H3 (A13824) and anti-IL-1 $\beta$  (A1112) was obtained from ABclonal (Wuhan, China); anti- $\beta$ -catenin (66379-1-Ig) and anti-GAPDH (6004-1-Ig) was from Proteintech (Wuhan, China). Antibody of TGF- $\beta$ 1 was from Affinity (AF1027).

2.2. Patients

Kidney biopsy samples were obtained from CKD patients undergoing diagnostic evaluation at the Department of Nephrology, Children's Hospital of Nanjing Medical University (Nanjing, China). A total of 14 subjects (age range 1–14 years) were recruited for this study. The pathological diagnoses were IgA nephropathy (IgAN), sclerosing glomerulonephritis, anaphylactoid purpura nephritis (HSPN), thrombotic microangiopathy, lupus nephritis (LN), anti-neutrophil cytoplasmic antibodies (ANCA)-associated vasculitis (AAV), subacute tubulointerstitial nephropathy, or focal segmental glomerulosclerosis (FSGS). The patient information is summarized in Table 1. Non-tumor kidney tissue from patients with benign renal tumors and from those undergoing partial nephrectomy comprised the normal controls.

The use of patient biopsy samples and nephrectomy tissue was approved by the Human Experimentation Committee of Nanjing Medical University Children's Hospital (202206126-1). All patients provided written informed consent.

2.3. Animals and unilateral ureteral occlusion (UUO) model

Animal studies were undertaken at the Laboratory Animal Center of the Nanjing Medical University and all the mice were housed with unrestricted access to food and water in accordance with the procedures of the Institutional Animal Care and Use Committee of the Nanjing Medical University (IACUC-2102005).

**Table 1**  
The basic information and diagnosis of renal biopsy specimens.

Sex	Age (years)	Proteinuria (g/24 h)	Pathological diagnosis	Serum creatinine ( $\mu$ mol/L)	BUN (mmol/L)
Girl	12.2	6.62	IgAN (Lee IV)	81.5	6.08
Boy	1.3	–	Sclerosing glomerulonephritis	75.7	12.24
Boy	13.6	2.91	HSPN IIIa	91.0	4.00
Girl	1.5	–	Thrombotic microangiopathy	49	5.59
Boy	11.7	3.01	Sclerosing glomerulonephritis	41.0	3.60
Girl	14.0	0.95	LN V	46.2	4.48
Boy	13.8	0.10	IgAN (Lee III)	72	6.91
Boy	12.8	0.44	IgAN	67.6	5.46
Boy	11.1	1.35	IgAN (Lee III)	64.8	7.13
Girl	6.9	8.48	AAV	191.2	20.96
Boy	8.0	–	Subacute tubulointerstitial nephropathy	387.0	20.10
Girl	6.0	3.99	IgAN (Lee III)	76.5	6.83
Girl	10.8	2.72	AAV	272.0	21.30
Girl	11.8	–	FSGS	30.2	4.10

IgAN: IgA nephropathy; HSPN: Henoch-Schonlein purpura nephropathy; LN: lupus nephritis; AAV: ANCA-associated vasculitis; FSGS: focal segmental glomerulosclerosis.

To assess the effect of Apcin on CKD, a UUO model was established. Eight-week-old male C57BL/6J mice from the Laboratory Animal Center of the Nanjing Medical University were randomly divided into four groups. The animals were pretreated with Apcin (5 mg/kg/day) by intraperitoneal injection for 1 day. Then, the UUO surgery was performed as follows: Mice were anesthetized with isoflurane. The retroperitoneal area was opened by a subcostal lateral incision, the left kidney was exteriorized, the proximal ureter was ligated with 4-0 suture silk, the kidney was replaced, and the incision was closed and sutured. The other steps were identical in the sham group except for ureteral ligation. Apcin was administered continuously for the next 7 days before the animals were euthanized by exsanguination under isoflurane. Subsequently, the kidney tissue was fixed in 4 % paraformaldehyde for histological analysis, and the remaining was stored at –80 °C for mRNA and protein analysis.

2.4. Histological analysis

Kidney tissues were fixed in 4 % paraformaldehyde for at least 24 h and embedded in paraffin. Then, the paraffined kidney sections (3  $\mu$ m) were deparaffinized, rehydrated, and stained using Masson's trichrome staining to visualize the collagenous connective tissue fibers. The fibrosis area (blue) vs. total area was assessed quantitatively using Image ProPlus.

2.5. Immunohistochemical staining

For immunohistochemical staining, 3- $\mu$ m-thick paraffin-embedded kidney sections were incubated in 3 % hydrogen peroxide for 20 min and subjected to antigen retrieval using citrate antigen retrieval buffer (Beyotime, Shanghai, China) in boiling water for 20 min. Then, the sections were blocked with the immunostaining blocking solution (Beyotime) and incubated with CDC20 (1:100), FN 1 (1:200), and  $\alpha$ -SMA (1:300) antibodies overnight at 4 °C. The color reaction was developed using diaminobenzidine (DAB), and the nuclei were counterstained with hematoxylin. The image analysis and quantification were performed using Image ProPlus.

## 2.6. Cell culture

Renal fibroblast cells (NRK-49F, CRL-1570™) and Mouse kidney proximal tubular epithelial cells (mPTC, CRL-3361™) were from ATCC. NRK-49F cells were maintained in DMEM containing 10 % FBS and mPTC cells were cultured in DMEM: F12 containing 7 % FBS and 6 mg/L insulin (Beyotime) at 37 °C under 5 % CO<sub>2</sub> and subcultured at 50–80 % confluency using 0.25 % trypsin-0.02 % EDTA (Invitrogen, Carlsbad, CA, USA). In some experiments, cells were pretreated with Apcin (25 or 50 nM) for 0.5 h or transfected with CDC20 plasmids for 6 h and then treated with recombinant human TGF-β1 (10 ng/mL for NRK-49F or 15 ng/mL for mPTC cells) for 24 h.

## 2.7. Cell proliferation and cytotoxicity assays

Cell viability was determined using CCK-8 assay.  $1 \times 10^4$  of NRK-49F and  $5 \times 10^3$  of mPTCs were seeded in 96-well plates and treated with various concentrations of Apcin (0–200 nM). After culturing for 24 h, 10 μL of CCK-8 reagent was added to each well and incubated for 1–2 h. The absorbance was measured at 450 nm on a microplate reader (OD-1000+, Onedrop™, Nanjing, China).

## 2.8. Quantitative real-time polymerase chain reaction (qPCR)

Total RNA was isolated from tissues or cells using TRIzol (Invitrogen) according to the manufacturer's instructions. cDNA was synthesized from 1 μg of RNA using HiScript II RT supermix (Vazyme, Nanjing, China). Then, qPCR was performed using SYBR Green PCR Master Mix (Vazyme, Nanjing, China) on a LightCycler 96 Instrument (Roche, Mannheim, Germany). GAPDH was used as a housekeeping control to normalize the target gene expression using the ΔΔCt method (Table 2).

## 2.9. Western blot analysis

Cells or tissues were lysed in RIPA buffer containing protease inhibitor cocktail (Roche) and boiled for 10 min. An equivalent of 20 μg/lane protein was separated on 10 % sodium dodecyl sulfate-polyacrylamide gel electrophoresis (SDS-PAGE) and electroblotted to polyvinylidene fluoride (PVDF) membranes (Immobilon, Millipore, Bedford, MA, USA). The membranes were blocked with 5 % nonfat milk in Tris-buffered saline (20 mM Tris-HCl and 0.5 M NaCl, pH 7.5) for 1 h and incubated overnight with antibodies against FN1 (1:1000), collagen type I (1:1000), collagen type III (1:1000), α-SMA (1:2000), CDC20 (1:1000), β-catenin (1:5000), Snail (1:1000), Histone H3 (1:1000), IL-1β (1:1000), TGF-β1 (1:1000) and GAPDH (1:10,000) at 4 °C. The immunoreactive bands were visualized using the Biosciences enhanced

chemiluminescent (ECL) detection system (Amersham, Little Chalfont, UK). The densitometric analysis was performed using Image J software (NIH, <https://imagej.nih.gov/ij>).

## 2.10. Nuclear and cytoplasmic fractionation

Cells were cultured in 6-well plates overnight and treated with TGF-β1 for 24 h with or without CDC20 overexpression. The cytoplasmic and nuclear extracts were isolated using the Thermo Scientific™ NE-PER™ Nuclear and Cytoplasmic Extraction Reagents (Cat. No. 78833, Thermo Scientific, Waltham, MA, USA), according to the manufacturer's instructions. Western blot analysis was performed as described above.

## 2.11. Statistical analysis

Results are expressed as mean ± standard error of the mean (SEM). Differences between the two groups were analyzed using a two-tailed Student's *t*-test, and the graphs were drawn using GraphPad Prism 6 software (GraphPad Software). One-way analysis of variance (ANOVA) was used for comparisons among multiple groups. *P*-values <0.05 indicated a statistically significant difference.

## 3. Results

### 3.1. Enhanced CDC20 was correlated with the degree of fibrosis

To explore the role of CDC20 in CKD, we firstly investigated the expression of CDC20 in biopsy samples from CKD patients at different stages of renal interstitial fibrosis. Immunohistochemical results showed that CDC20 was expressed at low levels in the renal tubules and renal interstitium of normal human kidneys but increased significantly in CKD patients (Fig. 1A and B). This phenomenon was confirmed by the double staining of CDC20 and lotus tetragonolobus lectin (LTL, a marker of proximal renal tubules) (Fig. 1D) or FSP1 (a marker of fibroblasts) (Fig. 1E). Importantly, the level of CDC20 expression was positively correlated with the degree of kidney fibrosis, based on the fibrosis score ( $r = 0.620$ ,  $P < 0.001$ ; Fig. 1C). Moreover, in a renal fibrosis animal model (unilateral ureteral obstruction, UUO), Western blot analysis confirmed that CDC20 levels were significantly increased in obstructed kidneys (Fig. 1F and G). These data indicated that CDC20 might be involved in renal fibrosis.

### 3.2. CDC20 inhibitor Apcin ameliorated UUO-induced renal fibrosis

Fibrosis is the final common pathway and the histological manifestation of CKD. To further elucidate the role of CDC20 in renal fibrosis, we conducted UUO surgery on C57BL/6J mice to establish the renal fibrosis model. Mice were pretreated with CDC20 inhibitor Apcin until euthanized on day 7. The therapeutic doses of Apcin showed no obvious toxicity on kidney, liver, and heart (Supplemental Fig. S1). Compared to sham-operated mice, renal fibrosis detected by Masson's trichrome and Sirius red staining for collagen showed that Apcin significantly reduced collagen deposition and fibrotic lesions in the renal interstitium (Fig. 2A–C).

In order to confirm whether UUO-induced renal fibrosis was reduced in Apcin-treated group, we examined the expression of FN1, Collagen I, and Collagen III. The results of immunohistochemical staining showed that UUO-induced FN1 expression was significantly reduced in the Apcin-treated group (Fig. 2D and E). Apcin significantly decreased the mRNA levels of Collagen I and Collagen III that were elevated following UUO injury (Fig. 2H and I). Western blotting results further confirmed that both Collagen I and Collagen III were significantly attenuated in the Apcin+UUO group (Fig. 2J and K). The profibrotic factor TGF-β1 also decreased after Apcin treatment (Fig. 2J and K). Apcin did not affect the expression of CDC20 possibly because Apcin competently inhibits CDC20 activity by binding to CDC20, but not affects CDC20 protein

**Table 2**

The sequences of the primers used in the study.

Primer name	Primer sequence 5'-3'
rFN1-F	TGGGACTGTACCTGCATTGG
rFN1-R	CCCAGCAGCGTGATCAAAAC
rCollagenI-F	GTGCTCTGTTATTTGCTGGT
rCollagenI-R	GACCTTGAAGTCCAGCAGGG
rCollagenIII-F	CACCCCTCTCTTATTTTGGCAC
rCollagenIII-R	AGACTCATAGGACTGACCAAGGTAGTT
rGAPDH-F	ATGATTCTACCCACGGCAAG
rGAPDH-R	CTGGAAGATGGTGATGGGTT
mFN1-F	CGTGGAGCAAGAAGGACAA
mFN1-R	GTGAGTCTGCGGTTGGTAAA
mα-SMA-F	CCCTGAAGAGCATCCGACA
mα-SMA-R	CCAGAGTCCAGCACAAATACC
mCollagenI-F	TAAGGGTCCCCAATGGTGAGA
mCollagenI-R	GGGTCCCTCGACTCCTACAT
mCollagenIII-F	AGGCAACAGTGGTTCTCTCTG
mCollagenIII-R	GACCTCGTGCTCCAGTTAGC
mGAPDH-F	GTCTTCACTACCATGGAGAAGG
mGAPDH-R	TCATGGATGACCTTGGCCAG

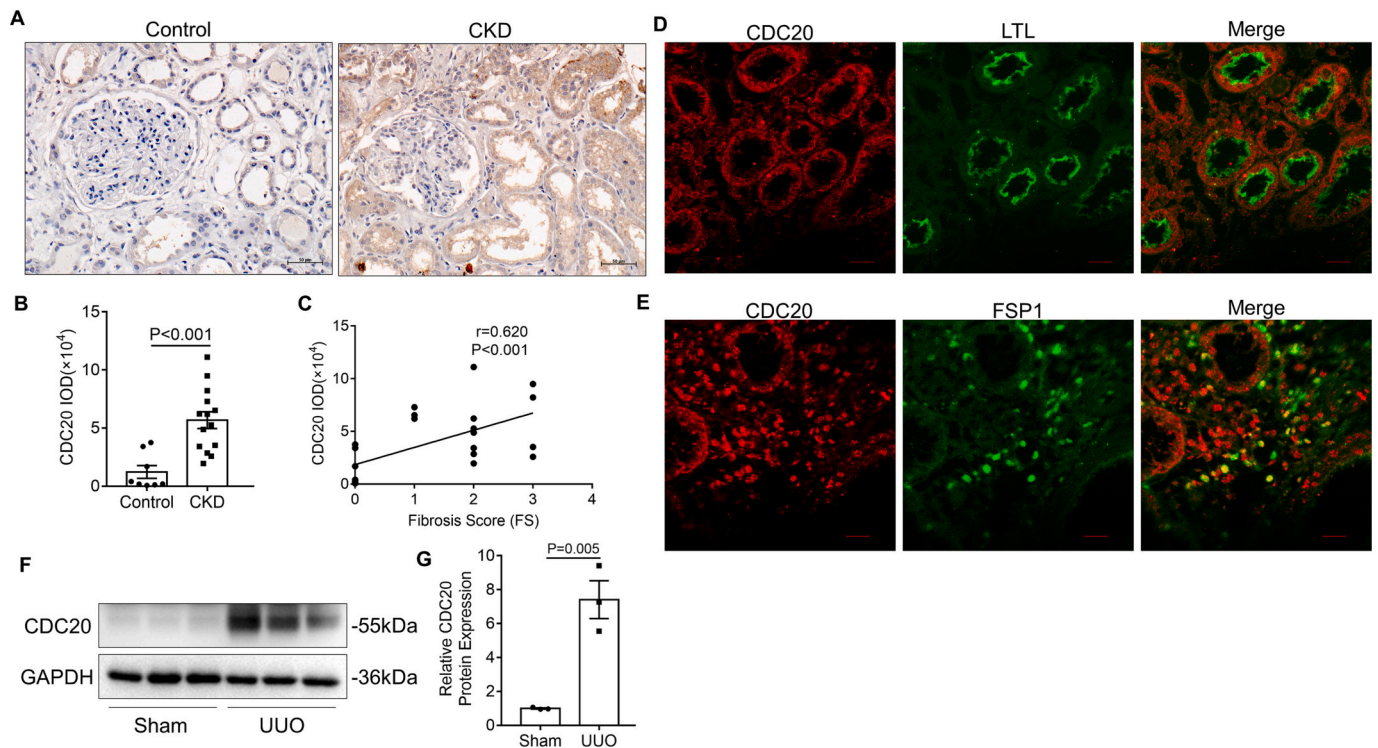


**Fig. 1.** Enhanced CDC20 was correlated with the degree of fibrosis. (A and B) Representative micrographs showing CDC20 expression in kidney biopsy specimens from CKD patients with fibrosis ( $n = 14$ ). Adjacent nontumor kidney tissue from patients who had renal cell carcinoma was used as control. Scale bar: 50  $\mu\text{m}$ . Image analysis and quantification were performed using Image-Pro Plus. (C) Linear regression showing renal CDC20 is positively correlated with the extent of fibrosis in CKD patients. The Spearman correlation coefficient ( $r$ ) and P value are shown. (D) Colocalization of CDC20 and LTL (a specific proximal tubule marker) in kidneys from CKD patients. Scale bar: 20  $\mu\text{m}$ . (E) Colocalization of CDC20 and FSP1 (a specific fibroblast marker) in kidneys from CKD patients. Scale bar: 20  $\mu\text{m}$ . (F and G) Western blot and quantitative data showing renal expression of CDC20 in sham-operated and UUO mice ( $n = 3$ ). The values represent means  $\pm$  SEM.

expression (Fig. 2J and K). These data provided strong evidence that Apcin attenuates UUO-induced ECM accumulation.

Fibroblasts and myofibroblasts are the final executors of renal fibrosis. These activated executors can produce substantial ECM, leading to fibrosis. Myofibroblasts are the activated form of fibroblasts, characterized by the expression of alpha-smooth muscle actin ( $\alpha$ -SMA) [22]. As shown in Fig. 2, the expression level of  $\alpha$ -SMA was significantly increased in the UUO model, as shown by immunohistochemical staining (Fig. 2F and G). Additional Apcin treatment attenuated the increase of  $\alpha$ -SMA expression.

Inflammation also plays an important role in the progression of CKD. Therefore, we also examined the inflammatory state in the obstructed kidneys of UUO mice. As shown by western blotting analysis, UUO significantly induced the expression of inflammatory factor interleukin-1 $\beta$  (IL-1 $\beta$ ), which was significantly inhibited by administration of Apcin (Supplemental Fig. S2).

### 3.3. Apcin reduced TGF- $\beta$ 1-induced ECM production in mPTC cells

Although fibroblasts are the major contributors to renal fibrosis, recent studies have shown that renal tubular epithelial cells can generate mature deposited ECM upon stimulation by TGF- $\beta$ 1 [23]. Therefore, we wondered whether Apcin reduces TGF- $\beta$ 1-induced ECM accumulation in mPTC cells. First, we determined that exposing mPTCs to Apcin did not cause a significant decrease in cell viability in a concentration-dependent manner (Fig. 3A). TGF- $\beta$ 1 was administered 0.5 h after Apcin treatment. In the current study, both 25 nM and 50 nM Apcin administrations notably reduced the TGF- $\beta$ 1-induced elevation of FN1, Collagen I, and Collagen III (Fig. 3B–D). Western blotting further confirmed that 50 nM Apcin treatment conspicuously reduced the expression of FN1 and Collagen III compared to the TGF- $\beta$ 1-stimulated

group (Fig. 3E and F). Consistent with in vivo results, Apcin did not affect CDC20 expression in mPTC cells (Fig. 3E and F).

### 3.4. Apcin diminished TGF- $\beta$ 1-mediated fibroblast activation

Next, we examined the role of Apcin in fibroblast activation. In NRK49F cells, Apcin treatment only slightly decreased the cell viability at high concentrations (10.11 %) (Fig. 4A), indicating that Apcin does not affect the growth of fibroblasts under physiological conditions. Western blot and qPCR analysis showed that the administration of Apcin prior to TGF- $\beta$ 1 stimulation significantly decreased the levels of FN1 and Collagen III (Fig. 4B, C, D, and E). The expression of CDC20 increased after TGF- $\beta$ 1 stimulation, which was not significantly affected after Apcin treatment (Fig. 4D and E). These data confirmed that Apcin reduces TGF- $\beta$ 1-induced fibroblast activation in NRK49F cells.

### 3.5. CDC20 deteriorated TGF- $\beta$ 1-induced ECM production in mPTC cells

Although inhibition of CDC20 reduces UUO- and TGF- $\beta$ 1-induced renal fibrosis, it is unclear whether CDC20 induces renal fibrosis. Next, we overexpressed CDC20 in mPTC cells (Fig. 5A) and observed a conspicuous increase in TGF- $\beta$ 1-induced ECM secretion. In cells treated with TGF- $\beta$ 1, markedly increased FN1,  $\alpha$ -SMA, and Collagen I mRNA levels were observed following CDC20 overexpression (Fig. 5B–D). Western blot and semi-quantitative analysis confirmed that CDC20 overexpression further induces the protein levels of FN1,  $\alpha$ -SMA, and Collagen III after TGF- $\beta$ 1 treatment (Fig. 5E and F).

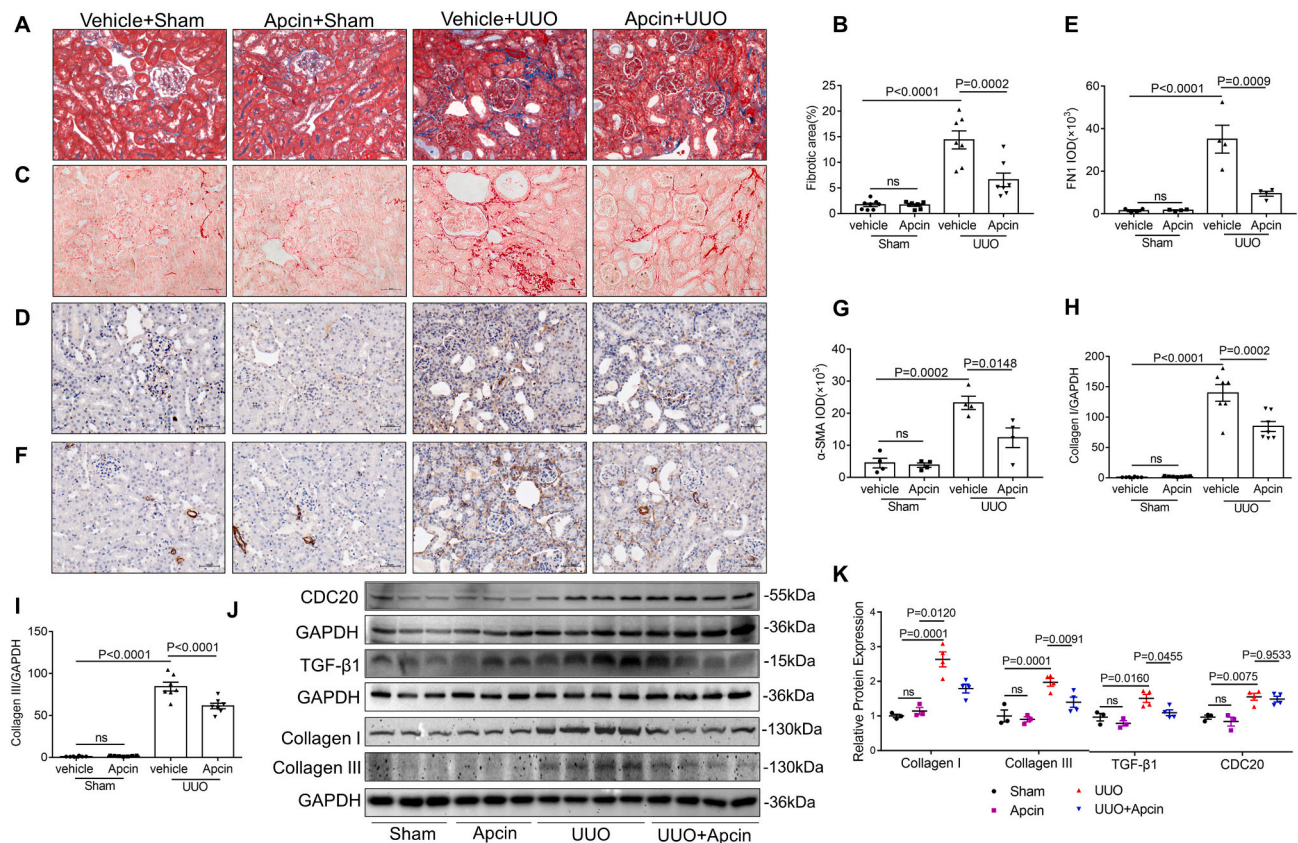


**Fig. 2.** CDC20 inhibitor Apcin ameliorated UUO-induced renal fibrosis. (A) Representative micrographs showing collagen deposition in obstructed kidneys. Mice were pretreated with Apcin (5 mg/kg per day) by intraperitoneal injection for 1 day. UUO surgery was then performed, and Apcin was administered continuously for the next 7 days until mice were sacrificed on day 7. Paraffin sections were subjected to Masson's trichrome staining for collagen deposition. Scale bar: 50  $\mu$ m. (B) Graphic presentation showing the fibrotic area in kidney tissues among groups as indicated (n = 8 in vehicle Sham group; n = 7 in Apcin Sham group; n = 7 in vehicle UUO group; n = 7 in Apcin UUO group). The quantification of fibrotic area was performed by Image-Pro Plus. (C) Representative micrographs of Sirius red staining in mice after UUO. Scale bar: 50  $\mu$ m. (D and E) Representative micrographs and quantitative data for FN1 immune staining in kidney tissues (n = 4). Scale bar: 50  $\mu$ m. (F and G) Representative micrographs and quantitative data showing  $\alpha$ -SMA expression in kidney tissues among groups as indicated (n = 4). Scale bar: 50  $\mu$ m. Positive signal quantification was performed using Image-Pro Plus. (H and I) The mRNA level of Collagen I and Collagen III were evaluated by qRT-PCR (n = 8 in vehicle Sham group; n = 7 in Apcin Sham group; n = 7 in vehicle UUO group; n = 7 in Apcin UUO group). (J and K) Representative Western blot and quantitative data showing renal expression of Collagen I, Collagen III, TGF- $\beta$ 1 and CDC20 (n = 3 in sham group; n = 4 in UUO group). The values represent means  $\pm$  SEM. P values were shown in figure.

### 3.6. CDC20 aggravated TGF- $\beta$ 1-induced fibroblast activation in NRK49F cells

To further validate the role of CDC20 in fibroblasts, we overexpressed CDC20 in NRK49F cells, followed by TGF- $\beta$ 1 stimulation. Notably, Collagen III and FN1 protein levels were elevated in cells that overexpressed CDC20 following TGF- $\beta$ 1 stimulation (Fig. 6A–C), as well as the mRNA levels of FN1 and Collagen I (Fig. 6D and E).

### 3.7. CDC20 regulated nuclear translocation of $\beta$ -catenin

CDC20 is associated with the cell cycle regulation. Thus, we examined cell cycle status in renal tubular cells and fibroblasts with TGF- $\beta$ 1 stimulation after CDC20 overexpression or inhibition with Apcin. We found that modulation of CDC20 did not affect the cell cycle progression, suggesting that the role of CDC20 in the present experimental setting was not associated with cell cycle regulation (Supplemental Fig. S3).

The Wnt/ $\beta$ -catenin signaling pathway plays a critical role in renal development; this system was suppressed in adulthood [24]. In a steady state,  $\beta$ -catenin is inactivated by a complex termed “destruction complex,” but can be re-expressed by injured kidneys and other tissues [25,26]. Subsequently,  $\beta$ -catenin is translocated into the nucleus, where it acts as a transcription factor to trigger Wnt-dependent gene expression

and ultimately promotes renal fibrosis [24]. The pathway analysis of CDC20-interacting proteins indicated that CDC20 plays additional roles outside of the cell cycle regulation process, including  $\beta$ -catenin pathway [27]. Reportedly, in colorectal cancer, CDC20 activates  $\beta$ -catenin by mediating the degradation of conductin via a conserved D-box domain [28]. Thus, we examined the activity of  $\beta$ -catenin in the UUO model, where it targets a significantly induced profibrotic *Snail* gene; this activation could be remarkably inhibited by Apcin (Fig. 7A and B). In vitro, the overexpression of CDC20 in tubular epithelial and NRK-49F cells increased the TGF- $\beta$ 1-induced nuclear translocation of  $\beta$ -catenin (Fig. 7C–F). These results suggested that the profibrotic effect of CDC20 may be achieved via  $\beta$ -catenin activation, which is summarized in Fig. 8.

## 4. Discussion

Fibrosis is an irreversible process responsible for the eventual progression of CKD to end-stage renal disease. Inhibiting this slow progression may be the key to improving the outcomes in CKD patients; however, the underlying mechanisms are yet unclear. Altered CDC20 expression has been reported in fibrosis in different organs. The upregulated expression of CDC20 has been observed in an inhalation model of chrysotile-induced fibrogenesis [29]. Several datasets also indicate a potential role of increased CDC20 expression in endometrial and liver

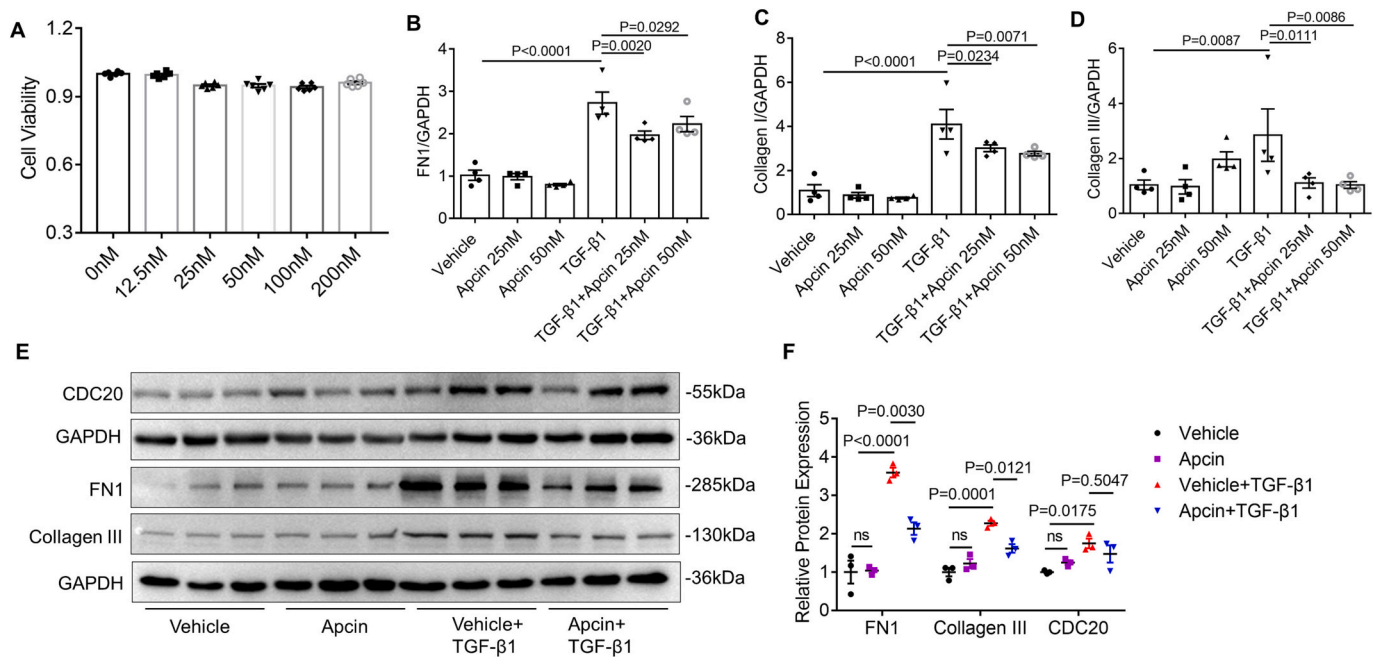


**Fig. 3.** Apcin reduced TGF-β1-induced extracellular matrix production in mPTC cells. The mPTC cells were pretreated with Apcin or DMSO for 0.5 h and then treated with recombinant human TGF-β1 (15 ng/mL) for 24 h. (A) Cell viability of mPTC cells treated with different concentrations of Apcin for 24 h (n = 6). (B–D) Representative qRT-PCR data showing the mRNA level of FN1, Collagen I and Collagen III (n = 4). (E and F) Immunoblot analyses and quantitative data showing the expression of Collagen I, FN1 and CDC20 in mPTC cells with or without 50 nM Apcin (n = 3). The values represent means ± SEM. P values were shown in figure.

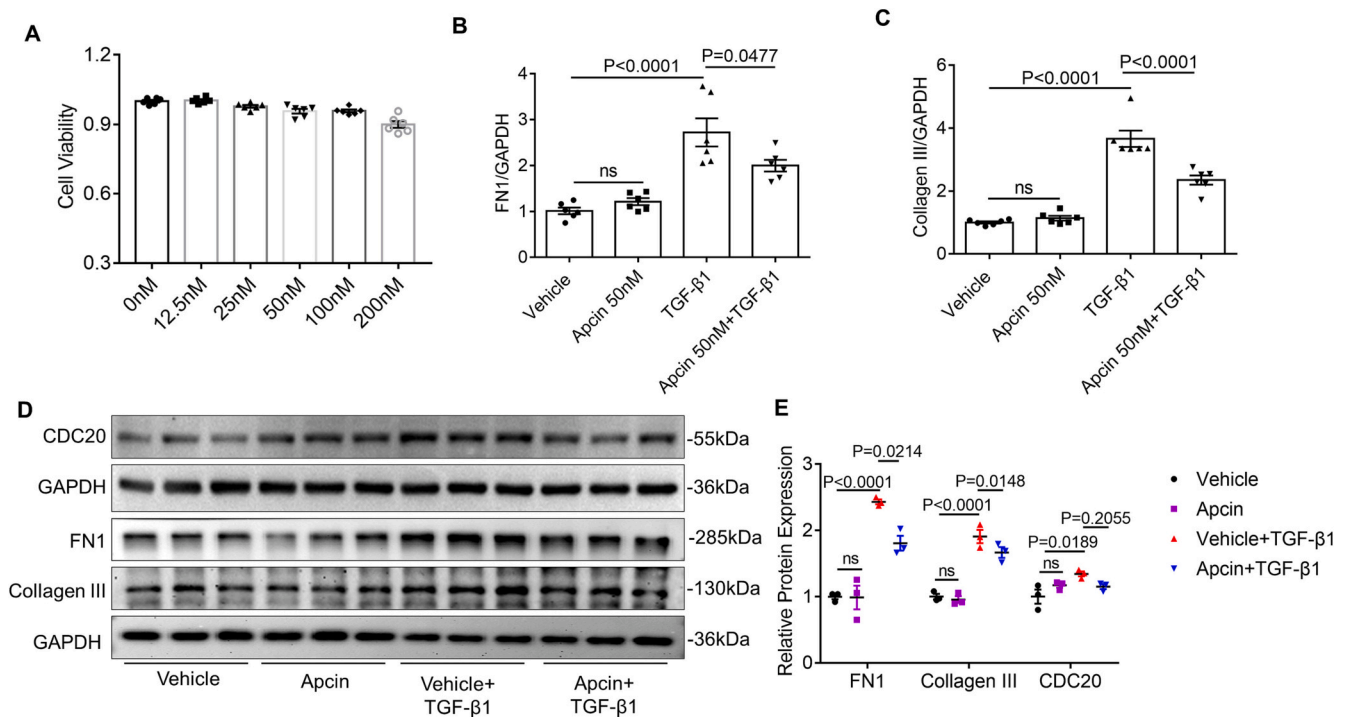


**Fig. 4.** Apcin blunted TGF-β1-mediated fibroblast activation. The NRK49F cells were pretreated with Apcin (50 nM or mentioned) or DMSO for 0.5 h and then treated with recombinant human TGF-β1 (10 ng/mL) for 24 h. (A) Cell viability of NRK49F cells treated with different concentrations of Apcin for 24 h (n = 6). (B and C) Quantitative determination of FN1 and Collagen III by qRT-PCR (n = 6). (D and E) Western blot and quantitative data showing Collagen III, FN1 and CDC20 protein levels (n = 3). The values represent means ± SEM. P values were shown in figure.

fibrosis [30,31]. However, the role of CDC20 in renal fibrosis has not been well-characterized. The present study showed that the expression of CDC20 was remarkably increased in both renal fibrosis patients and a mouse UUO model. Importantly, our data suggested a strong link between CDC20 expression and renal fibrosis.

The pathogenetic theories of renal fibrogenesis postulate a maladaptive repair process in response to various types of stimulation [32]. It is characterized by substantial histological changes that include forming fibroblastic foci and accumulating ECM components [33]. Previously, Apcin was identified as a CDC20 inhibitor exhibiting high

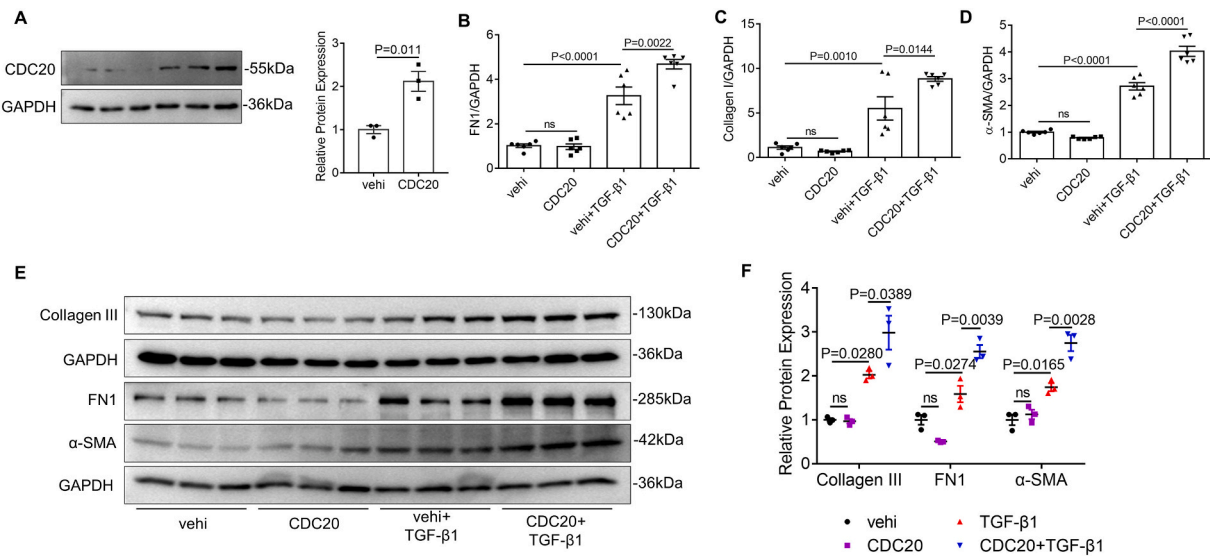


**Fig. 5.** CDC20 deteriorated TGF-β1-induced extracellular matrix production in mPTC cells. The mPTC cells were transfected with CDC20 plasmids and then treated with recombinant human TGF-β1 (15 ng/mL) for 24 h. (A) Western blot and quantitative data showing expression of CDC20 after CDC20 plasmids transfection (n = 3). (B–D) Representative qRT-PCR data showing the mRNA level of FN1, Collagen I and α-SMA (n = 6). (E and F) The expression of Collagen III, CDC20, α-SMA and FN1 in mPTC cells were detected by immunoblotting (n = 3). The values represent means ± SEM. P values were shown in figure.

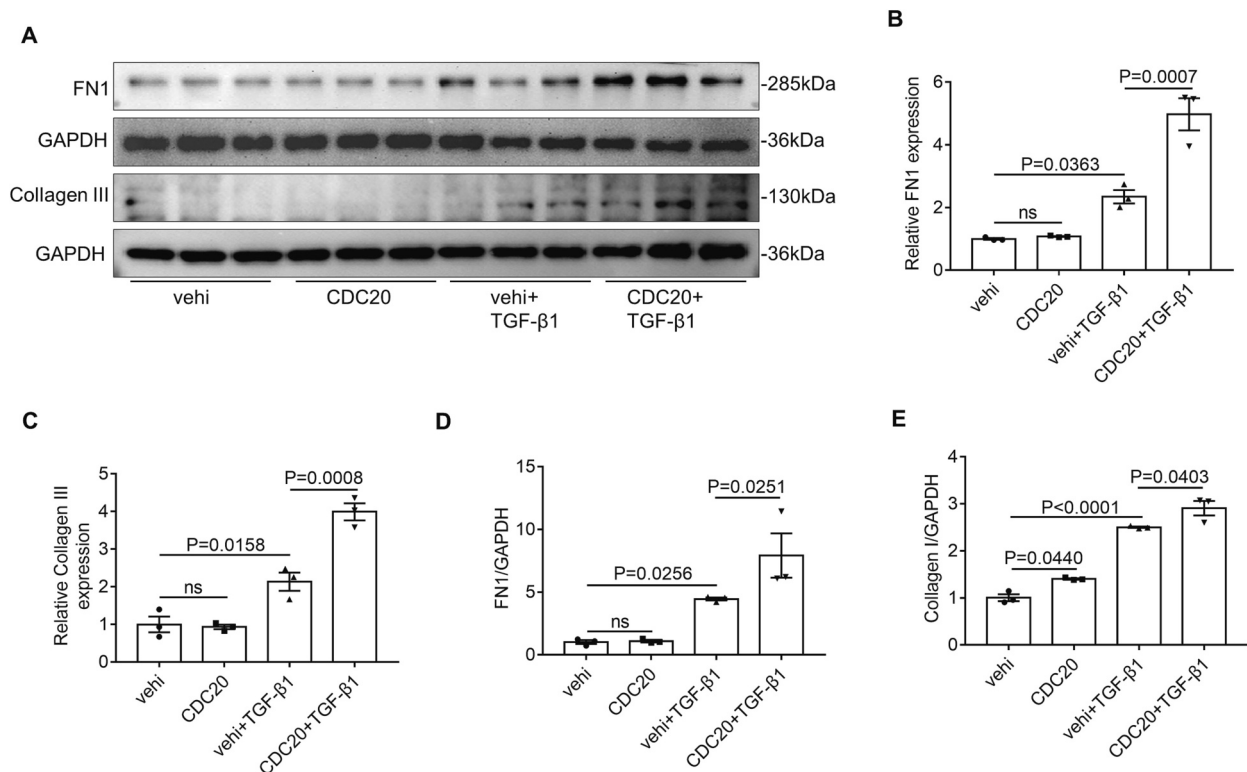


**Fig. 6.** CDC20 aggravated TGF-β1-induced fibroblast activation. The NRK49F cells were transfected with CDC20 plasmids and then treated with recombinant human TGF-β1 (10 ng/mL) for 24 h. (A–C) Western blot and quantitative data showing the expression of Collagen III and FN1 (n = 3). (D and E) The mRNA level of FN1 and Collagen I were evaluated by qRT-PCR (n = 3). The values represent means ± SEM. P values were shown in figure.

micromolar activities [34]. In the current study, Apcin-mediated inhibition of CDC20 was effective in attenuating UUO-induced fibrosis by reducing the renal deposition of ECM. Moreover, Apcin treatment abrogated the expression of α-SMA, a significant indicator of fibroblast activation [35]. All fibroblasts and myofibroblasts, especially myofibroblasts, expand in CKD and are major producers of ECM proteins [36]. Under physiological conditions, the inhibition of CDC20 did not

significantly affect the fibroblast growth in vitro. However, in TGF-β1-induced fibroblasts, CDC20 silencing significantly attenuated fibroblast activation and fibrotic deposition, which might be related to the increased expression of CDC20 and fibroblast expansion after fibrosis [37]. Strikingly, the inhibition of CDC20 might inhibit cell proliferation and induce cell cycle arrest in many hyperproliferative cells, such as glioblastoma cells and endometrial cells [12,38].

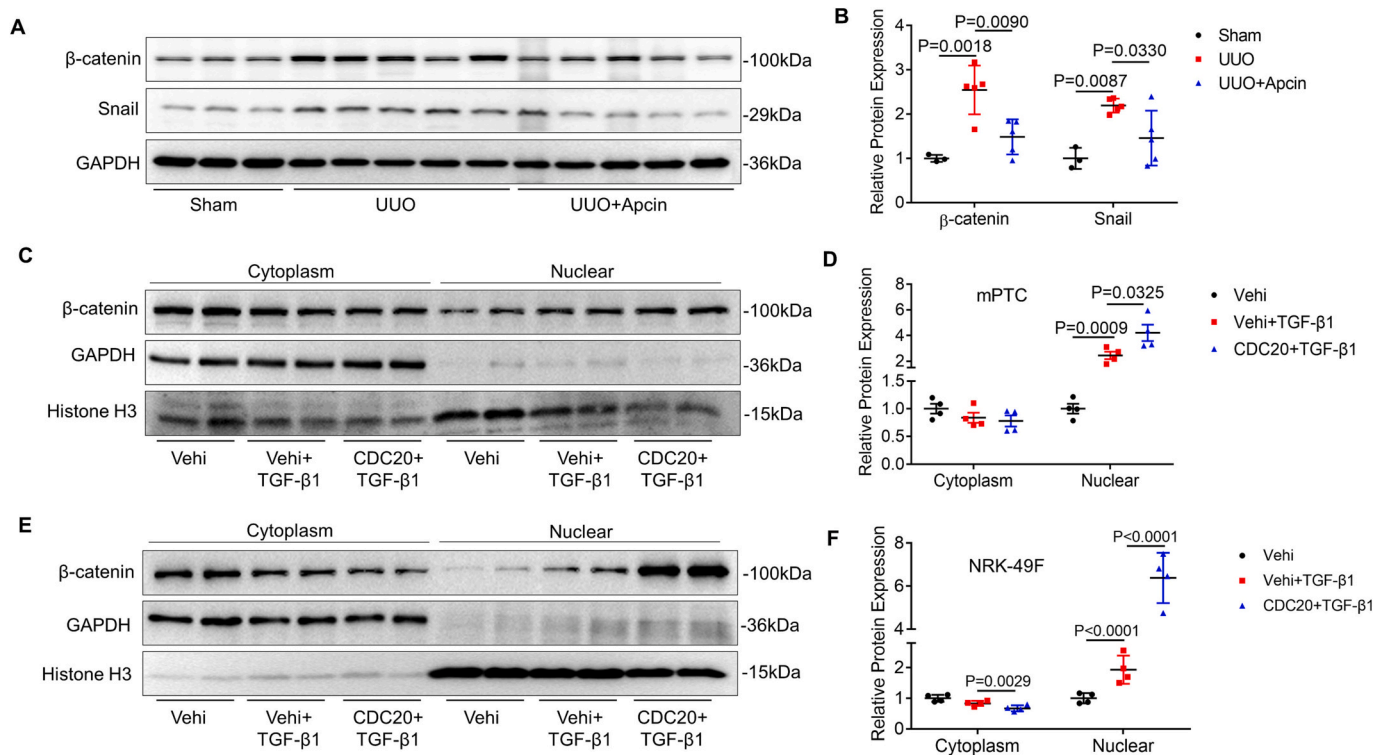


**Fig. 7.** CDC20 regulated nuclear translocation of β-catenin. (A and B) Western blot and quantitative analysis of β-catenin and Snail in UUO model with or without Apcin ( $n = 3$  in Sham group,  $n = 5$  in UUO and UUO + Apcin groups). (C and D) The mPTC cells were transfected with CDC20 plasmids and then treated with recombinant human TGF-β1 (15 ng/mL) for 24 h. Western blot and quantitative analysis of β-catenin in cytoplasm and nuclear ( $n = 4$  in each group). (E and F) The NRK-49F cells were transfected with CDC20 plasmids and then treated with recombinant human TGF-β1 (10 ng/mL) for 24 h. Western blot and quantitative analysis of β-catenin in cytoplasm and nuclear ( $n = 4$  in each group). The values represent means  $\pm$  SEM. P values were shown in figure.

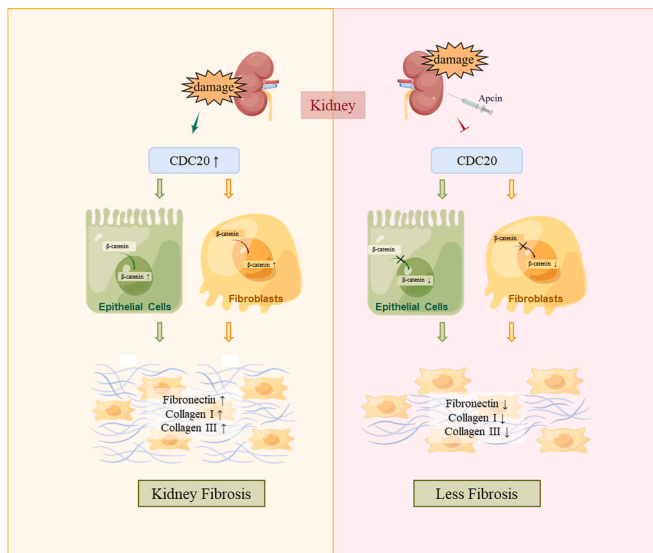


**Fig. 8.** Schematic for CDC20 aggravating the fibrotic response of renal tubular epithelial cells and fibroblasts by regulating the nuclear translocation of β-catenin in the mouse model of CKD.

Accumulating evidence has shown that tubular epithelial cells are not only victims of tubulointerstitial fibrosis but also initiators of fibrotic responses to various injuries [39–41]. Although the ECM genes were only slightly upregulated in epithelial cells, injured proximal renal tubular cells showed a high expression of ECM genes [36]. Similar to fibroblasts, Apcin also did not inhibit the growth of normal renal tubular epithelial cells but ameliorated the fibrotic process in these cells.

Surprisingly, since CDC20 is a key protein promoting anaphase during cell cycle progression, abolishing the expression of the protein raises the level of cyclin B1 that arrests the cell cycle in mitosis [42,43]. On the other hand, several studies have suggested that cell cycle arrest in renal tubular epithelial cells exacerbates renal fibrosis [44,45]. In our study, we found that CDC20 had no effect on the cell cycle progression in both renal tubular epithelial cells and fibroblasts, suggesting that CDC20 functioned independent of cell cycle mechanism in the present experimental setting.

Nevertheless, several indications support the possibility that CDC20 exacerbates fibrosis in epithelial cells. Reportedly, CDC20 inhibits β-catenin degradation in colorectal cancer cells [28]. The present study showed that Apcin significantly mediates the inhibition of β-catenin activity in UUO mice. The essential role of β-catenin activation in driving CKD progression has also been illustrated previously [46]. The activation of β-catenin triggers the transition of renal tubular epithelial cells to a mesenchymal phenotype [47] and modulates fibroblast-epithelial crosstalk [48]. Our results demonstrated that CDC20 increases nuclear translocation of β-catenin upon TGF-β1 stimulation in vitro. β-Catenin nuclear translocation activates the transcription of downstream profibrotic genes such as *Snail*, *c-Myc*, *PAII*, and *Twist*. Especially, *Snail* controls the major biological processes responsible for renal fibrogenesis activation but has also been reported to induce EMT and renal fibrosis in adult transgenic mice [49,50]. Also, in our study, the expression of *Snail* was decreased significantly along with the expression of β-catenin by the pharmacological inhibition of CDC20 in UUO mice. These data implied that CDC20 mediates renal fibrosis through the β-catenin pathway. However, the detailed mechanism of CDC20 in regulating the entry of β-catenin into the nucleus has not been investigated in this study. In addition, the upstream regulatory mechanism of CDC20 in this experimental setting was not explored. These limitations need to be addressed by further studies.

## 5. Conclusions

In the present study, we found that the increased level of CDC20 mediates extracellular matrix deposition and fibroblast activation in renal fibrosis. In addition, CDC20 inhibitor Apcin inhibits all these responses in vivo and in vitro. Furthermore, it was preliminarily shown that CDC20 accelerates fibrosis through  $\beta$ -catenin signaling. This is the first study on CDC20 and its inhibitor in renal fibrosis. Next, we functionally validated CDC20 in both renal tubular epithelial cells and mesenchymal fibroblasts, wherein it plays a major role in tubulointerstitial fibrosis. This effectively complements the mechanism of tubulointerstitial fibrosis and provides a putative therapeutic approach.

## Funding

This study was supported by the National Natural Science Foundation of China (82090020, 82090022, 82170689, 82070701, 81830020, 81873599).

## CRediT authorship contribution statement

**Jia He:** Formal analysis, Investigation, Writing – original draft. **Shuang Xu:** Validation, Investigation, Methodology. **Mingzhu Jiang:** Investigation, Methodology. **Ting Wang:** Methodology. **Yue Zhang:** Investigation. **Zhanjun Jia:** Supervision, Writing – review & editing. **Mi Bai:** Conceptualization, Supervision, Writing – original draft. **Aihua Zhang:** Conceptualization, Supervision, Writing – review & editing.

## Declaration of competing interest

The authors declare no conflicts of interest, financial or otherwise.

## Data availability

Data will be made available on request.

## Appendix A. Supplementary data

Supplementary data to this article can be found online at <https://doi.org/10.1016/j.bbadis.2023.166663>.

## References

- [1] C.P. Kovesdy, Epidemiology of chronic kidney disease: an update 2022, *Kidney Int. Suppl.* 12 (2022) (2011) 7–11.
- [2] J. Zhong, H.C. Yang, A.B. Fogo, A perspective on chronic kidney disease progression, *Am. J. Physiol. Ren. Physiol.* 312 (2017) F375–F384.
- [3] M. Ruiz-Ortega, S. Rayego-Mateos, S. Lamas, A. Ortiz, R.R. Rodriguez-Diez, Targeting the progression of chronic kidney disease, *Nat. Rev. Nephrol.* 16 (2020) 269–288.
- [4] T.D. Hewitson, Renal tubulointerstitial fibrosis: common but never simple, *Am. J. Physiol. Ren. Physiol.* 296 (2009) F1239–F1244.
- [5] R.D. Bulow, P. Boor, Extracellular matrix in kidney fibrosis: more than just a scaffold, *J. Histochem. Cytochem.* 67 (2019) 643–661.
- [6] M. Kapanidou, N.L. Curtis, V.M. Bolanos-Garcia, Cdc20: at the crossroads between chromosome segregation and mitotic exit, *Trends Biochem. Sci.* 42 (2017) 193–205.
- [7] B. Li, W.W. Xu, X.Y. Guan, Y.R. Qin, S. Law, N.P. Lee, K.T. Chan, P.Y. Tam, Y.Y. Li, K.W. Chan, H.F. Yuen, S.W. Tsao, Q.Y. He, A.L. Cheung, Competitive binding between Id1 and E2F1 to Cdc20 regulates E2F1 degradation and thymidylate synthase expression to promote esophageal cancer chemoresistance, *Clin. Cancer Res.* 22 (2016) 1243–1255.
- [8] A. Belur Nagaraj, O. Kovalenko, R. Avelar, P. Joseph, A. Brown, A. Surti, S. Mantilla, A. DiFeo, Mitotic exit dysfunction through the deregulation of APC/C characterizes cisplatin-resistant state in epithelial ovarian cancer, *Clin. Cancer Res.* 24 (2018) 4588–4601.
- [9] C. Alfieri, L. Chang, Z. Zhang, J. Yang, S. Maslen, M. Skehel, D. Barford, Molecular basis of APC/C regulation by the spindle assembly checkpoint, *Nature* 536 (2016) 431–436.
- [10] M.E. Harley, L.A. Allan, H.S. Sanderson, P.R. Clarke, Phosphorylation of Mcl-1 by CDK1-cyclin B1 initiates its Cdc20-dependent destruction during mitotic arrest, *EMBO J.* 29 (2010) 2407–2420.
- [11] L. Wan, M. Tan, J. Yang, H. Inuzuka, X. Dai, T. Wu, J. Liu, S. Shaik, G. Chen, J. Deng, M. Malumbres, A. Letai, M.W. Kirschner, Y. Sun, W. Wei, APC(Cdc20) suppresses apoptosis through targeting bim for ubiquitination and destruction, *Dev. Cell* 29 (2014) 377–391.
- [12] C. Guo, F. Kong, Y. Lv, N. Gao, X. Xiu, X. Sun, CDC20 inhibitor apcin inhibits embryo implantation in vivo and in vitro, *Cell Biochem. Funct.* 38 (2020) 810–816.
- [13] O. Shalom, N. Shalva, Y. Altschuler, B. Motro, The mammalian Nek1 kinase is involved in primary cilium formation, *FEBS Lett.* 582 (2008) 1465–1470.
- [14] Y. Du, M. Zhang, X. Liu, Z. Li, M. Hu, Y. Tian, L. Lv, X. Zhang, Y. Liu, P. Zhang, Y. Zhou, CDC20 promotes bone formation via APC/C dependent ubiquitination and degradation of p65, *EMBO Rep.* 22 (2021), e52576.
- [15] L. Wang, J. Zhang, L. Wan, X. Zhou, Z. Wang, W. Wei, Targeting Cdc20 as a novel cancer therapeutic strategy, *Pharmacol. Ther.* 151 (2015) 141–151.
- [16] F. Wu, Y. Sun, J. Chen, H. Li, K. Yao, Y. Liu, Q. Liu, J. Lu, The oncogenic role of APC/C activator protein Cdc20 by an integrated pan-cancer analysis in human tumors, *Front. Oncol.* 11 (2021), 721797.
- [17] L. Hu, M. Ding, W. He, Emerging therapeutic strategies for attenuating tubular EMT and kidney fibrosis by targeting Wnt/beta-catenin signaling, *Front. Pharmacol.* 12 (2021), 830340.
- [18] G. Yang, G. Wang, Y. Xiong, J. Sun, W. Li, T. Tang, J. Li, CDC20 promotes the progression of hepatocellular carcinoma by regulating epithelial-mesenchymal transition, *Mol. Med. Rep.* 24 (2021).
- [19] L. Wang, C. Yang, M. Chu, Z.W. Wang, B. Xue, Cdc20 induces the radioresistance of bladder cancer cells by targeting FoxO1 degradation, *Cancer Lett.* 500 (2021) 172–181.
- [20] J. Wang, F. Zhou, Y. Li, Q. Li, Z. Wu, L. Yu, F. Yuan, J. Liu, Y. Tian, Y. Cao, Y. Zhao, Y. Zheng, Cdc20 overexpression is involved in temozolomide-resistant glioma cells with epithelial-mesenchymal transition, *Cell Cycle* 16 (2017) 2355–2365.
- [21] K.L. Sackton, N. Dimova, X. Zeng, W. Tian, M. Zhang, T.B. Sackton, J. Meaders, K. L. Pfaff, F. Sigillot, H. Yu, X. Luo, R.W. King, Synergistic blockade of mitotic exit by two chemical inhibitors of the APC/C, *Nature* 514 (2014) 646–649.
- [22] R. Qi, C. Yang, Renal tubular epithelial cells: the neglected mediator of tubulointerstitial fibrosis after injury, *Cell Death Dis.* 9 (2018) 1126.
- [23] O.S. Qureshi, H. Bon, B. Twomey, G. Holdsworth, K. Ford, M. Bergin, L. Huang, M. Muzylak, L.J. Healy, V. Hurdowar, T.S. Johnson, An immunofluorescence assay for extracellular matrix components highlights the role of epithelial cells in producing a stable, fibrillar extracellular matrix, *Biol. Open* 6 (2017) 1423–1433.
- [24] S.J. Schunk, J. Floege, D. Fliser, T. Speer, WNT-beta-catenin signalling - a versatile player in kidney injury and repair, *Nat. Rev. Nephrol.* 17 (2021) 172–184.
- [25] J. Miao, J. Liu, J. Niu, Y. Zhang, W. Shen, C. Luo, Y. Liu, C. Li, H. Li, P. Yang, Y. Liu, F.F. Hou, L. Zhou, Wnt/beta-catenin/RAS signaling mediates age-related renal fibrosis and is associated with mitochondrial dysfunction, *Aging Cell* 18 (2019), e13004.
- [26] Y. Feng, J. Ren, Y. Gui, W. Wei, B. Shu, Q. Lu, X. Xue, X. Sun, W. He, J. Yang, C. Dai, Wnt/beta-catenin-promoted macrophage alternative activation contributes to kidney fibrosis, *J. Am Soc Nephrol* 29 (2018) 182–193.
- [27] S. Bruno, A. Ghelli, Luserna di Rora, R. Napolitano, S. Soverini, G. Martinelli, G. Simonetti, CDC20 in and out of mitosis: a prognostic factor and therapeutic target in hematological malignancies, *J. Exp. Clin. Cancer Res.* 41 (2022) 159.
- [28] M.V. Hadjihannas, D.B. Bernkopf, M. Bruckner, J. Behrens, Cell cycle control of Wnt/beta-catenin signalling by conductin/axin2 through CDC20, *EMBO Rep.* 13 (2012) 347–354.
- [29] T. Sabo-Attwood, M. Ramos-Nino, J. Bond, K.J. Butnor, N. Heintz, A.D. Gruber, C. Steele, D.J. Taatjes, P. Vacek, B.T. Mossman, Gene expression profiles reveal increased Mclca3 (Gob5) expression and mucin production in a murine model of asbestos-induced fibrogenesis, *Am. J. Pathol.* 167 (2005) 1243–1256.
- [30] J. Zhang, P. Jiang, Y. Tu, N. Li, Y. Huang, S. Jiang, W. Kong, R. Yuan, Identification and validation of long non-coding RNA associated ceRNAs in intrauterine adhesion, *Bioengineered* 13 (2022) 1039–1048.
- [31] Y. Lin, R. Liang, J. Ye, Q. Li, Z. Liu, X. Gao, X. Piao, R. Mai, D. Zou, L. Ge, A twenty gene-based gene set variation score reflects the pathological progression from cirrhosis to hepatocellular carcinoma, *Aging (Albany NY)* 11 (2019) 11157–11169.
- [32] Y. Sato, M. Takahashi, M. Yanagita, Pathophysiology of AKI to CKD progression, *Semin. Nephrol.* 40 (2020) 206–215.
- [33] S. Panizo, L. Martinez-Arias, C. Alonso-Montes, P. Cannata, B. Martin-Carro, J. L. Fernandez-Martin, M. Naves-Diaz, N. Carrillo-Lopez, J.B. Cannata-Andia, Fibrosis in chronic kidney disease: pathogenesis and consequences, *Int. J. Mol. Sci.* 22 (2021).
- [34] R. Verma, N.R. Peters, M. D'Onofrio, G.P. Tochtrop, K.M. Sakamoto, R. Varadan, M. Zhang, P. Coffino, D. Fushman, R.J. Deshaies, R.W. King, Ubistatins inhibit proteasome-dependent degradation by binding the ubiquitin chain, *Science* 306 (2004) 117–120.
- [35] A.V. Shinde, C. Humeres, N.G. Frangogiannis, The role of alpha-smooth muscle actin in fibroblast-mediated matrix contraction and remodeling, *Biochim. Biophys. Acta Mol. basis Dis.* 2017 (1863) 298–309.
- [36] C. Kuppe, M.M. Ibrahim, J. Kranz, X. Zhang, S. Ziegler, J. Perales-Paton, J. Jansen, K.C. Reimer, J.R. Smith, R. Dobie, J.R. Wilson-Kanamori, M. Halder, Y. Xu, N. Kabgani, N. Kaesler, M. Klaus, L. Gernhold, V.G. Puelles, T.B. Huber, P. Boor, S. Menzel, R.M. Hoogenboezem, E.M.J. Bindels, J. Steffens, J. Floege, R. K. Schneider, J. Saez-Rodriguez, N.C. Henderson, R. Kramann, Decoding myofibroblast origins in human kidney fibrosis, *Nature* 589 (2021) 281–286.
- [37] Q. Yuan, R.J. Tan, Y. Liu, Myofibroblast in kidney fibrosis: origin, activation, and regulation, *Adv. Exp. Med. Biol.* 1165 (2019) 253–283.
- [38] Y. Ding, C. Zhang, L. He, X. Song, C. Zheng, Y. Pan, S. Yu, Apcin inhibits the growth and invasion of glioblastoma cells and improves glioma sensitivity to temozolomide, *Bioengineered* 12 (2021) 10791–10798.

- [39] B.C. Liu, T.T. Tang, L.L. Lv, H.Y. Lan, Renal tubule injury: a driving force toward chronic kidney disease, *Kidney Int.* 93 (2018) 568–579.
- [40] L.L. Lv, Y. Feng, Y. Wen, W.J. Wu, H.F. Ni, Z.L. Li, L.T. Zhou, B. Wang, J.D. Zhang, S.D. Crowley, B.C. Liu, Exosomal CCL2 from tubular epithelial cells is critical for albumin-induced tubulointerstitial inflammation, *J Am Soc Nephrol* 29 (2018) 919–935.
- [41] S. Zhao, W. Li, W. Yu, T. Rao, H. Li, Y. Ruan, R. Yuan, C. Li, J. Ning, S. Li, W. Chen, F. Cheng, X. Zhou, Exosomal miR-21 from tubular cells contributes to renal fibrosis by activating fibroblasts via targeting PTEN in obstructed kidneys, *Theranostics* 11 (2021) 8660–8673.
- [42] S.S. Khumukcham, V.S.K. Samanthapudi, V. Penugurti, A. Kumari, P.S. Kesavan, L. R. Velatooru, S.R. Kotla, A. Mazumder, B. Manavathi, Hematopoietic PBX-interacting protein is a substrate and an inhibitor of the APC/C-Cdc20 complex and regulates mitosis by stabilizing cyclin B1, *J. Biol. Chem.* 294 (2019) 10236–10252.
- [43] V. Piano, A. Alex, P. Stege, S. Maffini, G.A. Stoppiello, P.J. Huis In 't Veld, I. R. Vetter, A. Musacchio, CDC20 assists its catalytic incorporation in the mitotic checkpoint complex, *Science* 371 (2021) 67–71.
- [44] B.C. Liu, T.T. Tang, L.L. Lv, How tubular epithelial cell injury contributes to renal fibrosis, *Adv. Exp. Med. Biol.* 1165 (2019) 233–252.
- [45] L.S. Gewin, Renal fibrosis: primacy of the proximal tubule, *Matrix Biol.* 68–69 (2018) 248–262.
- [46] S. Zhou, Q. Wu, X. Lin, X. Ling, J. Miao, X. Liu, C. Hu, Y. Zhang, N. Jia, F.F. Hou, Y. Liu, L. Zhou, Cannabinoid receptor type 2 promotes kidney fibrosis through orchestrating beta-catenin signaling, *Kidney Int.* 99 (2021) 364–381.
- [47] D. Zhou, R.J. Tan, L. Zhou, Y. Li, Y. Liu, Kidney tubular beta-catenin signaling controls interstitial fibroblast fate via epithelial-mesenchymal communication, *Sci. Rep.* 3 (2013) 1878.
- [48] S. Chen, M. Zhang, J. Li, J. Huang, S. Zhou, X. Hou, H. Ye, X. Liu, S. Xiang, W. Shen, J. Miao, F.F. Hou, Y. Liu, L. Zhou, Beta-catenin-controlled tubular cell-derived exosomes play a key role in fibroblast activation via the OPN-CD44 axis, *J. Extracell. Vesicles* 11 (2022), e12203.
- [49] A. Boutet, C.A. De Frutos, P.H. Maxwell, M.J. Mayol, J. Romero, M.A. Nieto, Snail activation disrupts tissue homeostasis and induces fibrosis in the adult kidney, *EMBO J.* 25 (2006) 5603–5613.
- [50] N. Simon-Tillaux, A. Hertig, Snail and kidney fibrosis, *Nephrol. Dial. Transplant.* 32 (2017) 224–233.